Geomechanics and Engineering, *Vol. 21, No. 2 (2020) 133-142*
DOI: https://doi.org/10.12989/gae.2020.21.2.133

Preliminary study on the ground behavior at shore connection of submerged floating tunnel using numerical analysis

Seok-Jun Kang[a], Jung-Tae Kim[a] and Gye-Chun Cho*

Department of Civil and Environmental Engineering, Korea Advanced Institute of Science and Technology, 291 Daehak-ro, Yuseong-gu, Daejeon 305-701, Republic of Korea

(Received December 4, 2019, Revised January 22, 2020, Accepted March 3, 2020)

Abstract. Submerged floating tunnel (SFT) is a type of tunnel which causes the tunnel segments to float in the water. When the SFTs are connected to the ground, the connection between the SFT and the subsea bored tunnel is fragile due to the difference in behavioral characteristics between the two types of tunnels. Therefore, special design and construction methods are needed to ensure the stability of the area around the connection. However, since previous research on the stability of the connection site has not been undertaken enough, the basic step necessitates the evaluation of ground behavior at the shore connection. In this study, the numerical analysis targeting the shore connection between the subsea bored tunnel and the SFT was simulated. The strain concentration at the shore connection was analyzed by numerical simulation and the effects of several factors were examined. The results showed the instability in the ground close to the shore connection due to the imbalance in the behavior of the two types of tunnels; the location of the strain concentration varies with different environmental and structural conditions. It is expected that the results from this study can be utilized in future studies to determine weak points in the shore connection between the submerged floating tunnel and the subsea bored tunnel, and devise methods to mitigate the risks.

Keywords: submerged floating tunnel; shore connection; numerical analysis; external load; grouting material; joint design

1. Introduction

Continuous globalization has increased the demand for maritime and air transport of humans and natural resources. Recently, subsea tunnels have become a major alternative to overcome the weaknesses of conventional ship and aircraft transport as they are less affected by environmental disasters. With the development of offshore geotechnical and structural technology, the concept of the submerged floating tunnel (SFT), which allows the creation of linear paths through the sea, has been proposed as a potential solution. To take advantage of the SFT and maximize its benefits, it is necessary to connect the tunnel path to an existing or artificial island. Ground connection is an economically suitable option for the necessary ventilation systems, emergency exits or rest areas, especially for long distance SFTs (Mazzolani *et al.* 2010). When the SFT is connected to an underground tunnel built inland, the two tunnels show different behaviors due to their different constraint conditions. The SFT moves dynamically due to the wave or traffic load (Yan *et al.* 2016) while the subsea bored tunnel has less displacement as it is prevented by the surrounding ground (Do *et al.* 2018). Since the two tunnels exhibit different behaviors, the stability of the shore connection has a great risk (Nilsen and Palmstrom 2001, Shi *et al.* 2016). Therefore, it is necessary to evaluate the safety at the shore connection, that must be designed with considering the behavioral characteristics of the tunnels in both environments. Depending on the nature of the marine environment in which the SFT is located and the nature of the ground where the underground tunnel is located, the design must be considered separately. Additionally, the structural characteristics of the two tunnels affect the safety at the connection. A typical supporting system of the SFT is composed of the tether and tunnel segment designs (Chen *et al.* 2008). Therefore, the design of the connection site between the subsea bored tunnel and the SFT should be performed considering the tunnel structure characteristics (Yarramsetty *et al.* 2019).

Previous research on the SFT mainly studied the behavior of the SFT under various conditions. Most research focused on the dynamic behavior of the tunnel when a dynamic load (wave, traffic load or seismic load) is applied assuming both ends of the floating tunnel are fixed (Kunish *et al.* 1994, Hong and Ge 2010, Youshi and Fei 2010). However, the dynamic response of the floating tunnel is affected by the boundary condition (Jin and Kim 2017), so considering the shore connection as the boundary condition is necessary. Some research has been done to propose the SFT segmentation method and the anchoring system (Jakobsen 2010, Zhang *et al.* 2010, Lee *et al.* 2017), but their design methods are suitable for immersed tunnels rather than floating tunnels. The degree of freedom at the connecting joint between tunnel segments was also considered as an important factor affecting the behavior of the SFT (Xiao and Huang 2010, Zhou *et al.* 2012, Oh *et al.*

*Corresponding author, Professor
E-mail: gyechun@kaist.ac.kr
[a]Ph.D. Student

ISSN: 2005-307X (Print), 2092-6219 (Online)

2013). However, they did not consider the characteristics of the ground surrounding the bored tunnel connected to the SFT. The studies related to the face stability of the tunnel at the shore connection (Nilsen and Palmstrom 2001, Zingg and Anagnostou 2012, Shi *et al.* 2016, Zhang *et al.* 2017) only considered the risks from seawater infiltration or ground strength reduction due to deep depth. These studies have investigated the risk at the connecting site, but have not considered the behavioral imbalance between the two types of tunnels. The efforts for actual practice of constructing the submerged floating tunnel has been conducted targeting Quiandao Lake, China (Mazzolani *et al.* 2010). The study designed the proto-type of the submerged floating tunnel considering the environment of Quiandao Lake and proposed the basic draft of the tunnel joint to prevent damage from earthquake or leakage. However, there was no consideration of the displacement imbalance between two types of tunnel. Overall, the previous studies did not consider the stability of the ground at the shore connection of the SFT, but suggested the important factors related to the behavior of the SFT. According to the result of the literature review, the main factors that must be considered are the marine environmental factor, the ground environmental factor and the structural factor.

In this study, the ground behavior at the shore connection between the SFT and the subsea bored tunnel is analyzed through three-dimensional numerical analysis. This is done to propose the risks arising at the shore connection in various conditions (Fig. 1). The type of external load acting on the SFT was considered as the main marine environmental factor affecting the safety on the shore connection. Therefore, the loading type, direction and location of application were controlled in the numerical simulation to evaluate their influence on the ground behavior at the shore connection. The grouting material surrounding the subsea bored tunnel and the joint design between the tunnel segments were adjusted as the structural factor in the simulation. Their effects on the ground behavior were evaluated through case study, varying the structural factors. As a result, there was strain concentration on the ground surrounding the shore connection regardless of applying various factors. The factors affect the size and location of the strain concentration. Although this study cannot establish clear criteria for the design of the shore connection at a specific target site, it contributes to understanding how the main factors affect the ground behavior around the shore connection. It is expected that the results can be utilized to predict weak points and to devise methods for reducing risks during the design process of the shore connection with the SFT.

2. Analysis method

2.1 Numerical software

Numerical analyses were performed to facilitate the analysis of relatively diverse cases to investigate the stability of the shore connection and the distribution aspect of the stress and displacement, rather than deriving quantitative results in a specific area. As a software for numerical simulation, Fast Lagrangian Analysis of Continuum in three dimensions (FLAC 3D) was used. FLAC 3D is used for geotechnical analysis, targeting factors including soil, rock, structures and supports. The main feature of FLAC 3D is its ease in analyzing the mechanism of continuum when applying civil or earth technology, and to simulate the ground behavior of large deformations, nonlinear materials or unstable conditions. Therefore, it is suitable for evaluating the behavior of the

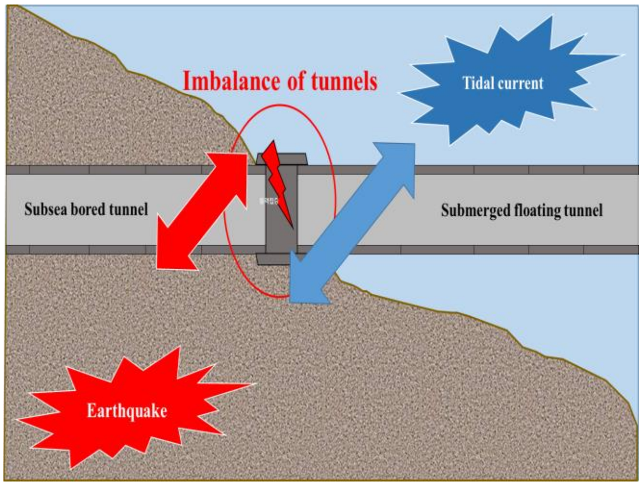

Fig. 1 Conceptual diagram of shore connection

Table 1 Rock properties

Rock type: Granite	
Density [kg/m^3]	2700
Elastic modulus [GPa]	40
Shear modulus [GPa]	16
Bulk modulus [GPa]	26.7
Friction angle [degrees]	30
Cohesion [MPa]	10
Tensile strength [MPa]	16

Table 2 Parameters for the numerical model

Parameter	Value
Tunnel diameter [m]	24
Segment thickness [m]	1.0
Water level [m]	100
Buoyancy to weight ratio	1.3

Table 3 Procedure of the numerical simulation

Step	Process
1	Formation of zones for initial ground
2	Application of gravity and water table to create initial state
3	Rock excavation for subsea bored tunnel
4	Installation of lining segments for SFT and bored tunnel
5	Simulation considering marine environment
6	Repeat with application of various conditions

ground and tunnel at the shore connection.

2.2 Numerical model

Numerical models consist of the ground, SFTs, subsea bored tunnels and marine environments. In order to investigate the influence of the environmental factors such as the external load, some parameters are assumed to be typical values. The ground was considered to be a homogeneous rock, and was modeled with the Mohr-Coulomb model. The rock properties with this model are assumed to be typical values of granite as shown in Table 1. The depth of the shore connection is assumed to be 100 m. During the actual construction, the depth of the connection between the SFT and the subsea bored tunnel depends on the characteristics of the construction site and the purpose of the construction. Thus, a sufficient depth for the effect of hydraulic pressure was chosen. The characteristics of the SFT and subsea bored tunnel depend on the purpose of the tunnel configuration and the wave strength of the target area. In this study, the tunnel size and concrete lining characteristics are assumed to be as presented in Table 2.

A numerical model that includes these assumptions is shown in Fig. 2. The boundary condition for the model was formed to prevent the outward displacement of cuboid ground by setting fixity in the vertical direction on the face of ground model. In order to prevent the boundary effect at the shore connection, the ground was formed such that the distance from the connection to the boundary is greater than five times the diameter of the tunnel. Numerical analysis was performed in the order listed in Table 3. The initial stress conditions were simulated after the ground and subsea environment were created. The pore water pressure and hydrostatic pressure were set to increase with depth considering the unit weight of water. After the construction of the initial state, the bored tunnel was excavated and the concrete lining was applied to prevent rock deformation. The SFT is directly connected to the subsea bored tunnel, following which the environmental factors acting on the SFT are applied. The buoyancy was applied on the SFT vertically upward with the magnitude calculated with buoyancy to weight ratio, 1.3.

2.3 Conditions for the numerical simulation

The numerical simulation was performed to evaluate the effect of various factors on the stability of the shore connection when the subsea bored tunnel and the SFT were connected. Initially, the distribution of the stress or displacement was investigated based on the analysis result without considering the main factors. Subsequently, the effects of each factor were analyzed by comparing the results from the changed factor with that of the initial analysis. The factors adjusted from the initial state include the characteristics of the external load acting on the submerged floating tunnel as a marine environmental factor, the tunnel-ground interface property and joint characteristics as the structural factors. The cases simulated to analyze the effects of the factors are summarized in Table 4. The dynamic load was applied in form of generated velocity at the end of the SFT. The frequency and magnitude of the dynamic movement are 0.5/sec and 1.0 m respectively. The dynamic behavior of the SFT transmitted through the tunnel and caused displacement throughout the whole floating tunnel.

Table 4 Numerical simulation cases

Initial state	Without external load or structural consideration
Marine environmental factor	Type of external load
	Direction of external load
	Location external load applied
Structural factor	Type of grouting material
	DOF configuration in tunnel joint
	Spacing of tunnel joint

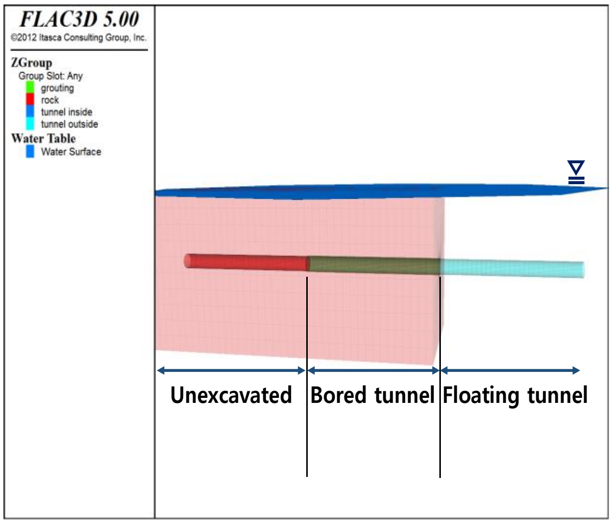

Fig. 2 Numerical model of the ground and tunnels

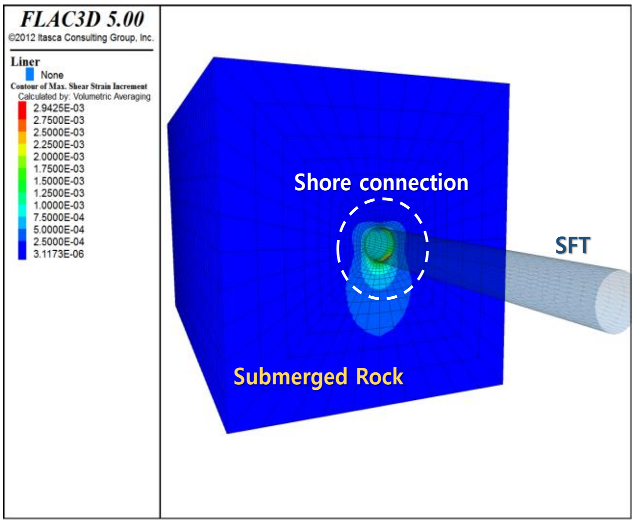

Fig. 3 Example of control case-shear strain rate (front view)

2.4 Initial state – control case

A case representing the initial state was simulated as a control case. This case simulates the two tunnels and the subsea ground environment with the exception of some

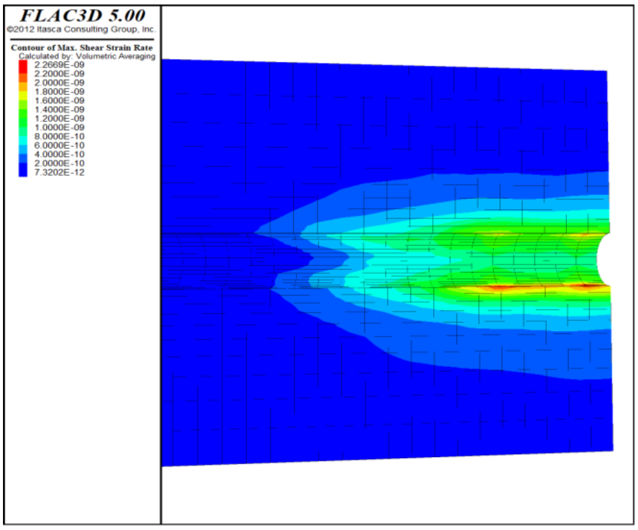

Fig. 4 Example of control case-shear strain rate (longitudinal view)

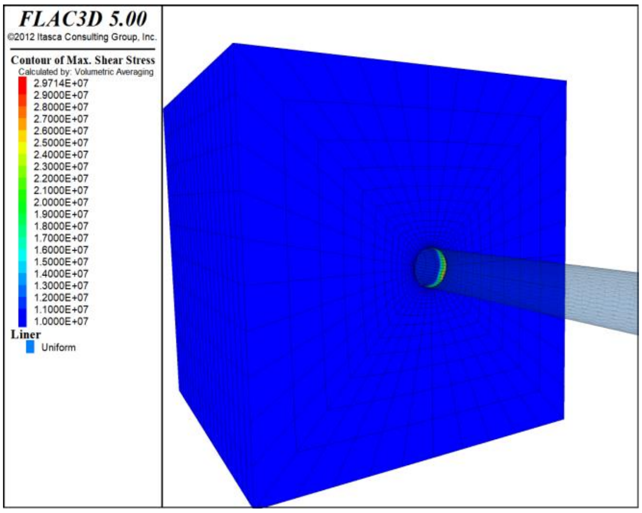

Fig. 5 Example of control case-shear stress (front view)

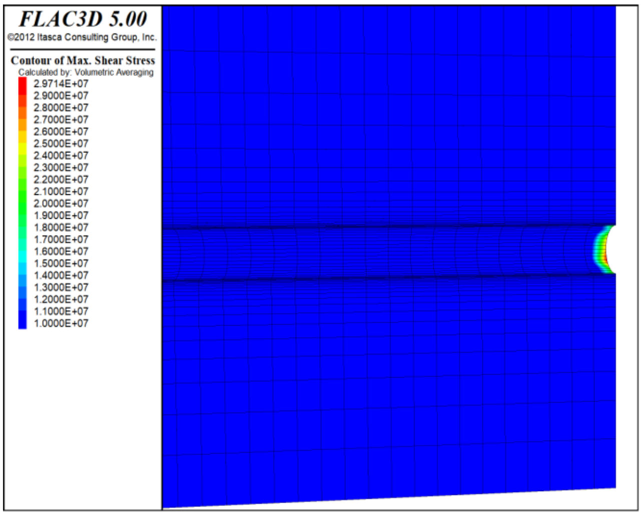

Fig. 6 Example of control case-shear stress (longitudinal view)

factors covered in the experimental group shown in Table 4.

The results from this control case were compared with those from the cases with changing factors. The results discussed in the following sections are derived by applying additional conditions or changing the values of factors from the initial state. Figs. 3 and 4 show the example of the analysis results of the control case. Although no external load is applied, shear strain is concentrated in the surrounding ground where the SFT and subsea bored tunnel are connected under the weight of the SFT. The following analytical results considering various factors focus on the stress and strain concentrations occurring in the ground around the shore connection highlighted by a white circle in Fig. 3. Fig. 4 expresses the longitudinal view of the simulation result. Figs. 5 and 6 show the shear stress distribution in the control case. Given the marine environment, the ground behavior under dynamic loads such as wave or traffic load should be analyzed. The stress distribution has difficulty in expressing the results from velocity occurred in a zone during an infinitesimal time using FLAC3D. It is more appropriate to understand the ground behavior through the distribution of strain rate according to the velocity of the zone. Therefore, the following numerical results are shown as a distribution of strain rates.

3. Effect of the external load

3.1 Type of external load

A Static load and dynamic load were applied on the SFT. For dynamic loads, the trigonometric load was utilized to simulate the wave load. The loads were input vertically downwards at the end of the floating tunnel. Since the static and dynamic load have different implications for the SFT stability, the locations of stress or strain concentration were compared for each load, rather than comparing quantitative results. Fig. 7 shows the vertical and axial strain distributions with two types of load. The results show that the sites of strain concentration are completely different in the two cases. Comparing the results with the control case (Figs. 7(a) and 7(d)), the static load acting on the SFT vertically causes the changes in magnitude or extent of the range with a similar strain concentration location as shown in Figs. 7(b) and 7(e). Conversely, in the case of the dynamic load, the strain concentration occurs at a different location. The vertical strain rate with the dynamic load in the ground is concentrated where the bored tunnel is located (Fig. 7(c)). The axial strain with the dynamic load (Fig. 7(f)) is concentrated at both sides as well as above and below the shore connection. The shear strain concentrated in the ground could be observed with the longitudinal view also (Fig. 8). The shear strain distributes through the ground surrounding the subsea bored tunnel, and the range of shear strain distributes widely when the static load was applied (Figs. 8(a) and 8(b)). According to these results, the location of the weak ground point depends on the type of external force applied on the SFT. Therefore, it is necessary to understand the type of external load to be applied on the SFT to consider the ground reinforcement.

3.2 Direction of external load

The ground behavior when the external load directions

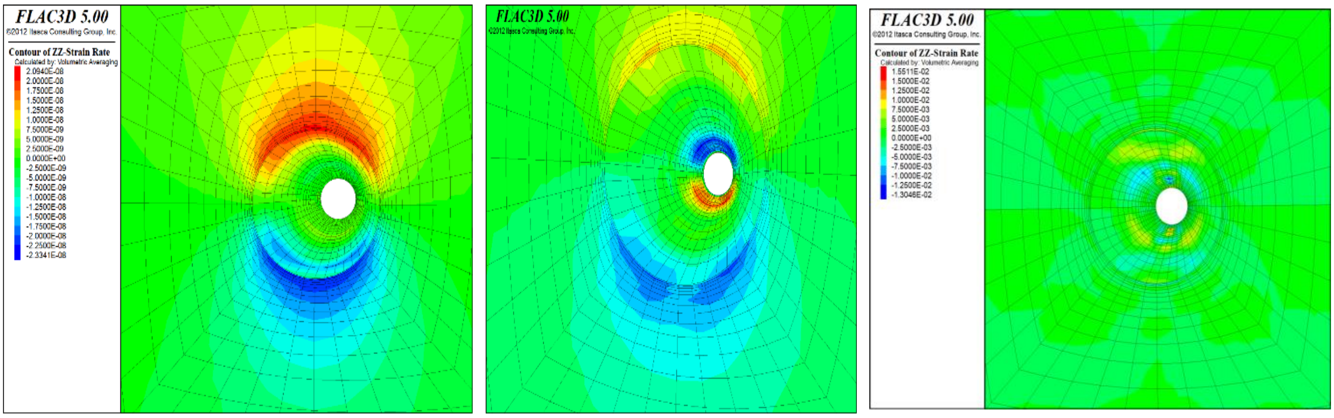

(a) Vertical strain without external load (b) Vertical strain with static load (c) Vertical strain with dynamic load

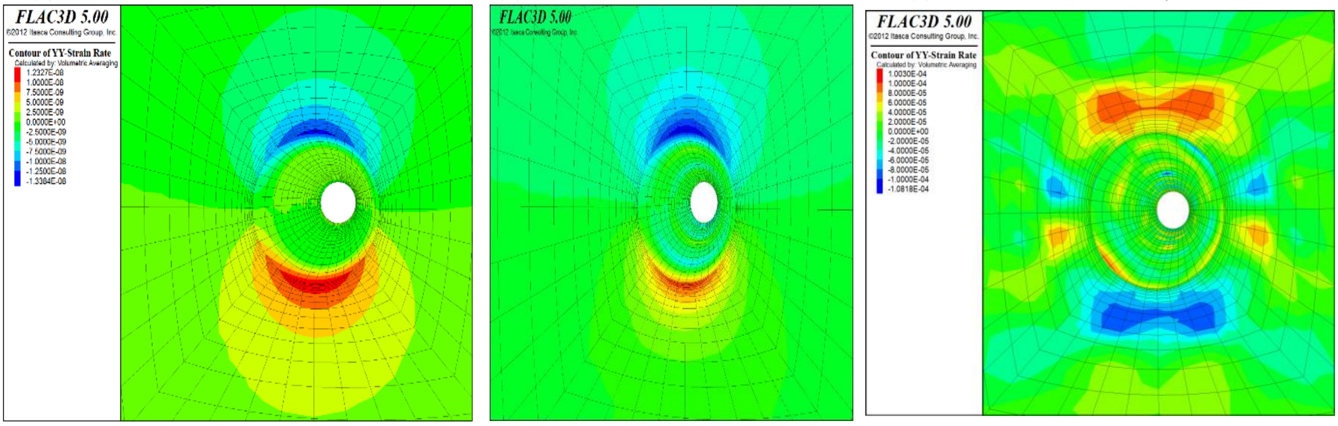

(d) Axial strain without external load (e) Axial strain with static load (f) Axial strain with dynamic load

Fig. 7 Distribution of vertical/axial strain in the ground surrounding the shore connection (front view)

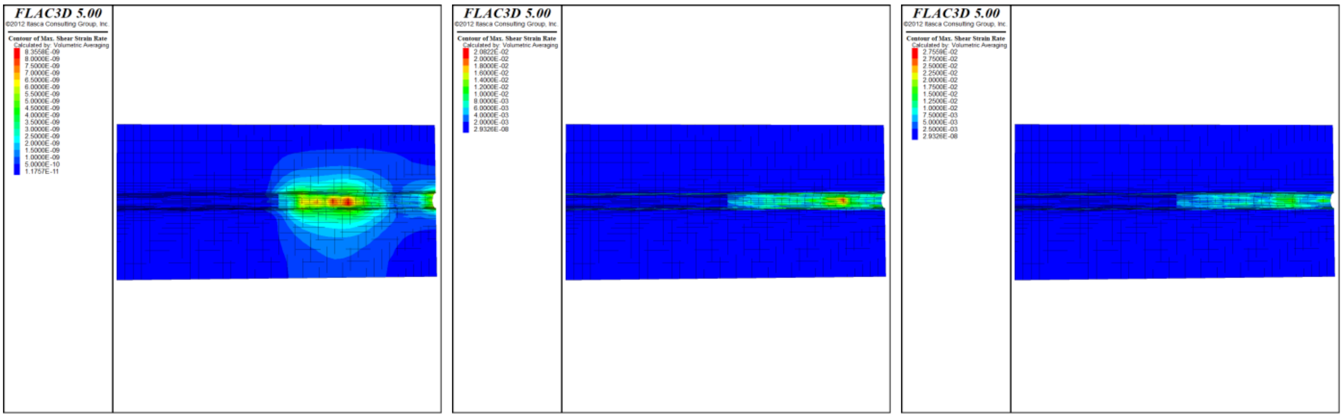

(a) Vertical static load (b) Vertical dynamic load (c) Horizontal dynamic load

Fig. 8 Distribution of shear strain in the ground surrounding the shore connection (longitudinal view)

of horizontal, vertical, and axial direction were applied has been analyzed. The location where the external loads are applied is fixed as the end point of the SFT, and the effect of applying direction is considered in the static and dynamic loading conditions. When the dynamic loads are applied, there is little change in the location of the shear strain concentration when the external load is applied horizontally or axially. Compared to the vertical dynamic load, the horizontal and axial loads cause the location of the shear strain concentration to move closer to the shore connection (Figs. 8(b) and 8(c)). The results of the static loads applied vertically upward, axially forward and axially backward show a slight influence on the strain distribution by the external load direction. Compared to Fig. 7(b) simulated with a vertically downward static load, only the extent of the strain distribution at the shore connection and the magnitude of the maximum strain are slightly affected with change in direction. Therefore, only the ground deformation near the shore connection and at the ends of the bored tunnel should be considered if only the static load is applied. However, the direction of the dynamic load application has to be carefully considered since it can cause the strain concentration in the middle of the bored tunnel.

3.3 Location of load application

The external load was applied on the floating tunnel at different locations. The locations where the external loads are applied were set in the middle and the end of the floating tunnel. When the static load is applied at different points, it slightly influences the magnitude or extent of distribution. However, there are changes in the strain distribution pattern when dynamic loads are applied. The external dynamic load in the axial and vertical directions are applied in the middle and the end of the floating tunnel. These results are compared with the results from cases that simulate the external dynamic loads applied in the end of the floating tunnel. The cases with the axial dynamic load show little change in the vertical strain distribution with change in the location of load application, and only the magnitude of maximum strain changes. Conversely, the location of the vertical strain concentration is closer to the shore connection when the vertical dynamic load is applied in the middle of the floating tunnel.

4. Effect of structural factors

4.1 Property of grouting material

In general, the grouting exists between the excavated ground and the tunnel segments to fill the gap. The behavior of the bored tunnel varies depending on the type of grouting material as shown in Figs. 9 and 10, indicating the numerical results with cement and clay grouting conditions. Therefore, understanding the interface characteristics between the tunnel and the grouting material and considering the characteristics for selecting the proper grouting material is essential. Simulations with various grouting materials were conducted to evaluate the effect of grouting material property on the ground behavior around the shore connection. The main property of the interface considered in the numerical model is the coupling stiffness. It is governed by the properties of grouting material surrounding the tunnel as expressed in Eq. (1) (Itasca 2013). The properties of the various grouting materials considered in the numerical simulations are shown in Table 5. The simulations were conducted with the condition that the vertical dynamic load is applied at the end of the floating tunnel.

As a result, the shear strain distributions with various grouting materials are shown in Figs. 11 and 12. Comparing with the shear strain distributions from Fig. 10, it is seen that the higher the stiffness of the material, the greater is the coupling stiffness acting on the interface between the tunnel and grouting material, and lower the deformation within the soil. The stiff grouting material resists deformation, so the shear stress transfers to the ground causing wide shear strain distribution as shown in the longitudinal view (Fig. 12). In addition, the results show that the location of shear strain concentration becomes closer with high stiffness of the grouting material. This tendency is expected to occur because the degree of stress that can be induced by grouting varies with the grouting material, and the stress applied on the ground changes.

Table 5 Properties of grouting materials

Type	Shear modulus [MPa]	Bulk modulus [MPa]	Coupling stiffness [GPa]
Clay	83	18	112
Material 1	1040	2300	1530
Material 2	2080	4600	3070
Material 3	3120	6900	4600
Cement	4160	9200	6130

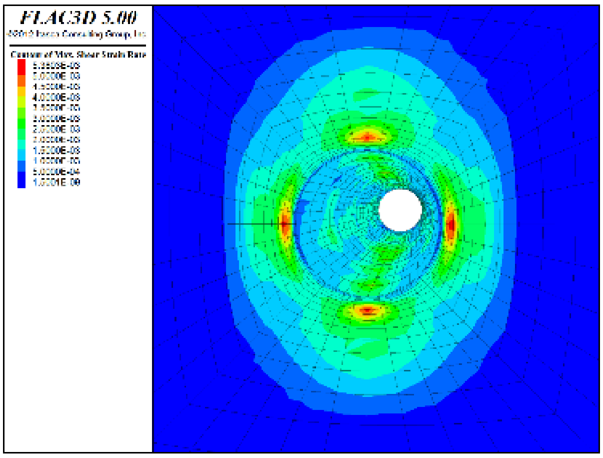

Fig. 9 Shear strain distribution with cement grouting

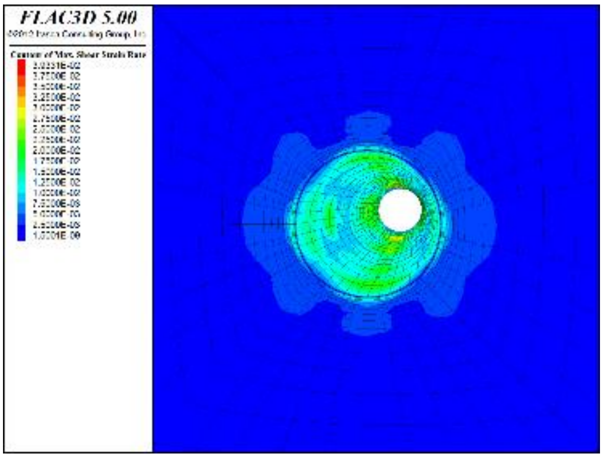

Fig. 10 Shear strain distribution with clay grouting

$$i_k = 100\frac{(K+\frac{4}{3}G)}{l_{min}}, \tag{1}$$

where i_k is coupling stiffness, K is bulk modulus, G is shear modulus, and l_{min} is minimum zone length.

4.2 Joint DOF configuration

When the stress and displacement from the submerged floating tunnel are transferred to the subsea bored tunnel, the ground behavior changes with the design of the joints of the two tunnels, which were analyzed by controlling the degree of freedom (DOF) in the joint. The DOF in the

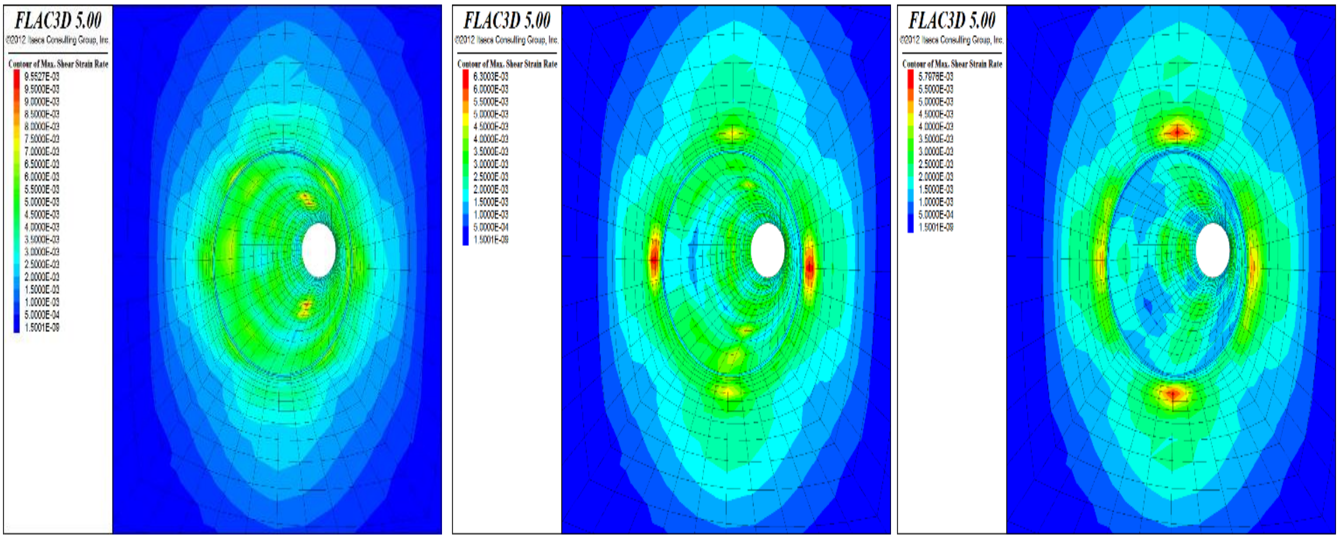

(a) Grouting material 1 (b) Grouting material 2 (c) Grouting material 3

Fig. 11 Shear strain distribution with various grouting materials (front view)

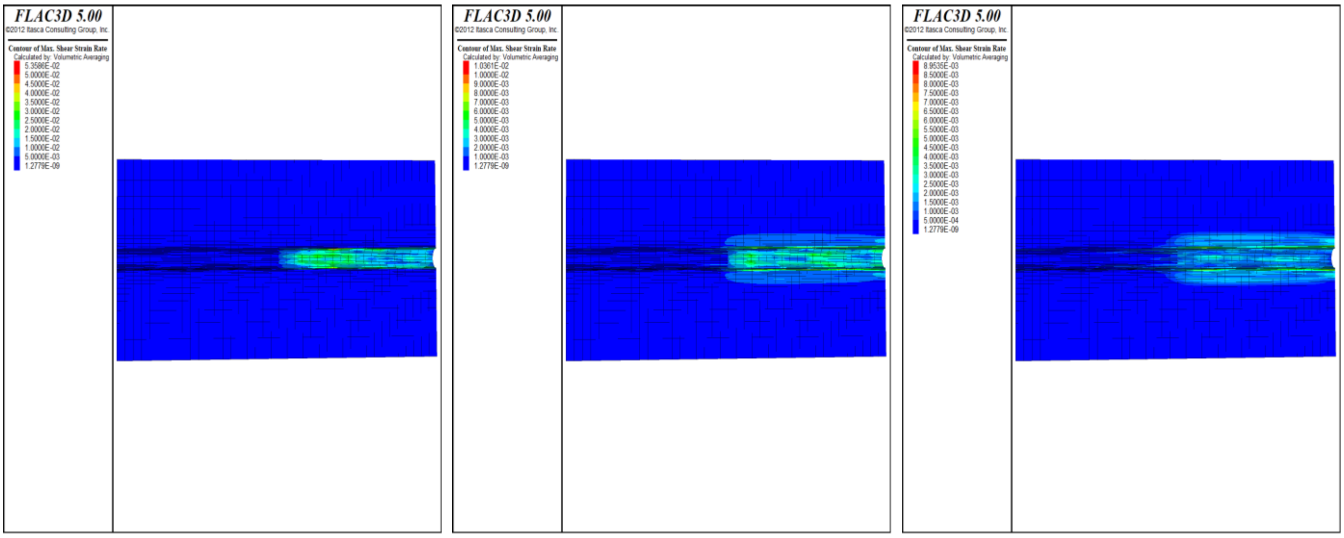

(a) Grouting material 1 (b) Grouting material 2 (c) Grouting material 3

Fig. 12 Shear strain distribution with various grouting materials (longitudinal view)

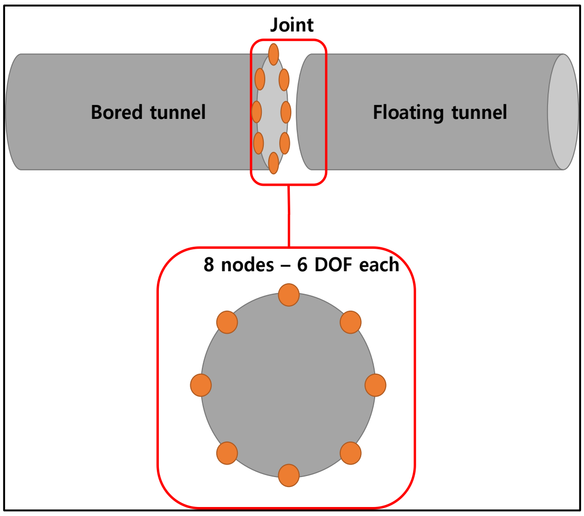

Fig. 13 Conceptual diagram for joint design

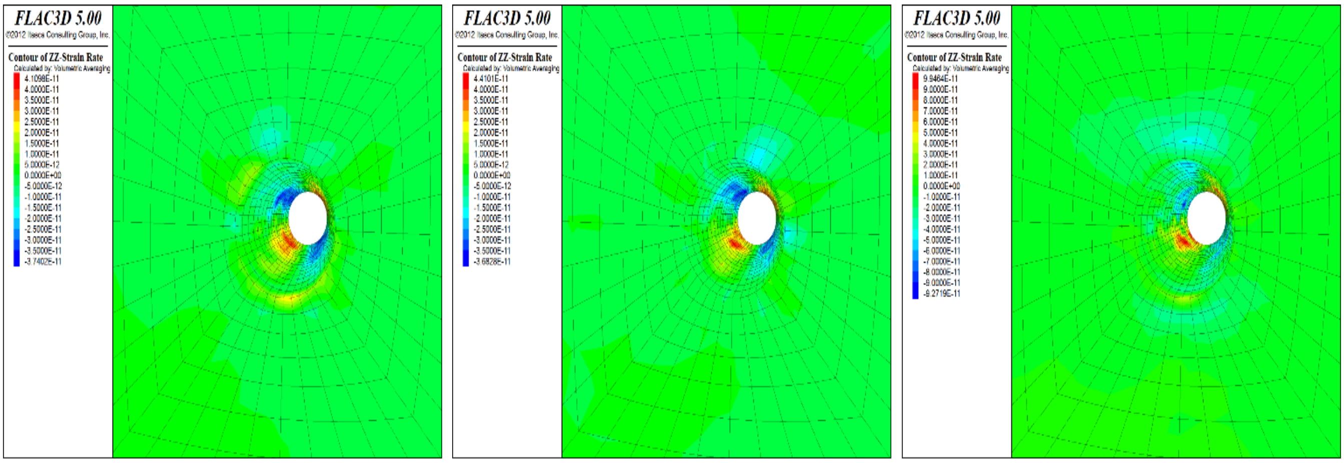

(a) Hinge (b) Hinge with axial deformation (c) Hinge with axial/vertical deformation

Fig. 14 Vertical strain distribution with various DOF in joint (front view)

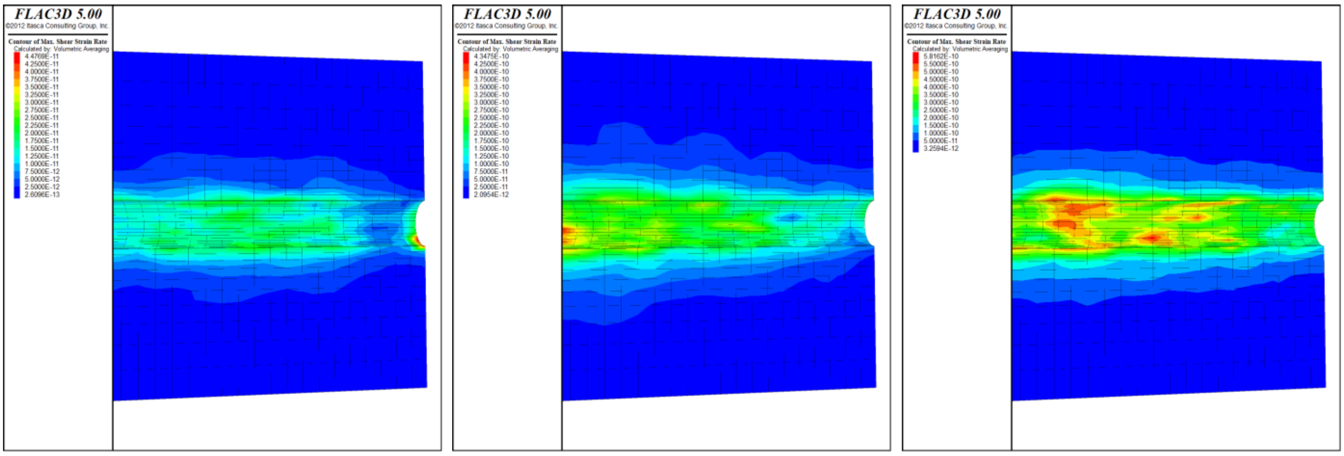

(a) Hinge (b) Hinge with axial deformation (c) Hinge with axial/vertical deformation

Fig. 15 Shear strain distribution with various DOF in joint (longitudinal view)

numerical analysis determines whether to allow deformation and rotation in the three axes in each node of the joint. A joint consists of 8 linkage nodes for the linkage between the tunnel segments. It connects the bored tunnel and the floating tunnel as shown in Fig. 13. Each linkage-node was set to have stiffness for displacement as well as free and rigid conditions. The joint designs as the DOF configuration were set as three cases: hinge, hinge allowing the axial deformation, hinge allowing the axial/vertical deformation. The results show that the range of strain concentration decreases by allowing additional deformation (Figs. 14 and 15). Compared to the case without allowing deformation and rotation at the joint (Fig. 7(b)), the strain concentration at the shore connection is resolved. The magnitude of vertical strain decreases significantly by allowing rotation at the connection of two tunnels. The strain concentration inside the bored tunnel decreases when additional deformation is allowed (Figs. 14(b) and 14(c)). However, the shear strain distributions in longitudinal view (Figs. 15(b) and 15(c)) show that more shear strain concentration occurs when axial and vertical deformation are allowed.

These results show that the joint DOF configuration can solve the problems caused by the strain concentration at the shore connection. The effect of the joint DOF configuration varies depending on the marine environmental factors. Thus, the optimal DOF configuration should be determined after evaluating the marine environmental factors of a target construction site.

4.3 Joint spacing

It was confirmed that the joint design with the DOF configuration at the connection of the two tunnels resolves the strain concentration at the shore connection. Subsequently, the analysis based on the joint spacing, which also means the number of joints installed in the bored tunnel segments, was conducted to examine the stability of the shore connection when the joint is added inside the bored tunnel. The cases of analysis consist of three conditions with joint spacing of 10, 20 and 50 m. Each joint has the DOF configuration that allows rotation, axial deformation and vertical deformation. The length of the bored tunnel is 100 m, so the number of joints is 10, 5 and 2 respectively in each case. The results showed that, the larger the number of joints, the lesser the ground deformation, as the joints between the tunnel segments deform and absorb more stress

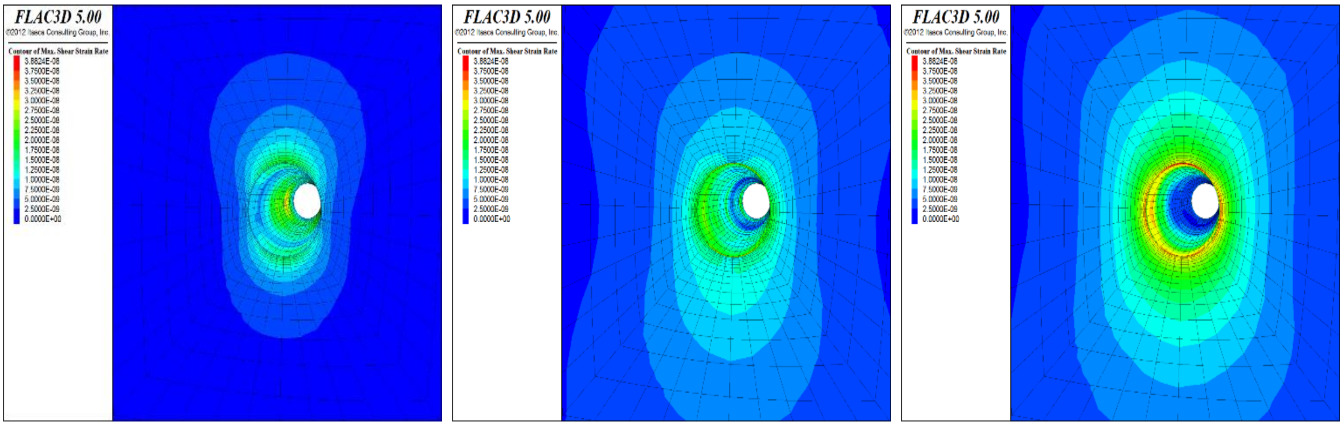

(a) 10 m spacing (b) 20 m spacing (c) 50 m spacing

Fig. 16 Shear strain distribution with various joint spacing (front view)

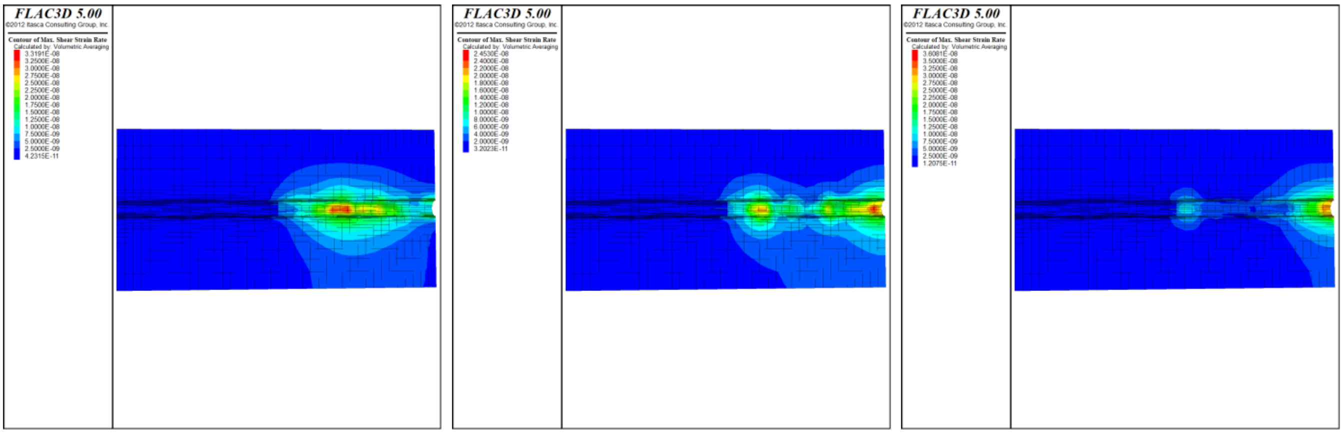

(a) 10 m spacing (b) 20 m spacing (c) 50 m spacing

Fig. 17 Shear strain distribution with various joint spacing (longitudinal view)

(Fig. 16). The deformation in the joint cause the shear strain spread through the ground as shown in the longitudinal view (Fig. 17). According to these results, the joint DOF configuration can be utilized in the subsea bored tunnel to relieve the stress transmitted from the submerged floating tunnel. Therefore, it is considered that the ground stability at the shore connection can be secured by adjusting the joint spacing based on the environmental conditions.

5. Conclusions

In this study, the numerical analysis to evaluate the ground behavior at the shore connection between the SFT and the subsea bored tunnel has been conducted. Considering various conditions, the strain distributions around the shore connection were analyzed on priority. Since this study was not conducted on exact target areas, it was conducted to determine the impact of the main factors on the shore connection of the SFT to propose the area to be considered for further study. The main conclusions derived from this study are summarized as follows:

• As the conditions of the two tunnels and submerged ground are simulated, the strain concentrations occur at shore connections even without external loads.

• When the static and dynamic loads are applied on the SFT, the tendencies of the strain concentration in both cases are completely different.

• The direction or location of the external loads applied on the SFT also affects the site where the strain is concentrated at the shore connection.

• The strain concentration at the shore connection can be resolved with low-stiffness grouting material, as the strain concentrated at the shore connection is widely transferred into the excavated ground.

• Structural design of the joint between the bored tunnel and the floating tunnel relieves the strain concentration at the shore connection.

• The degree of freedom at the nodes in the joint can be utilized to relieve the strain concentration based on the environmental conditions such as the external load.

• The joint spacing installed through the bored tunnel can be considered in the design step to secure the ground stability at the shore connection.

• These results can be used to understand the risks at the shore connection and to evaluate the effect of several factors on the ground behavior at the shore connection.

• Even though this study includes only qualitative results to understand the range of strain concentration, it is expected that the results can propose the areas that need consideration in future studies.

Acknowledgments

This work was supported by the National Research Foundation of Korea (NRF) grant funded by the Korea government (MSIT) (No. 2017R1A5A1014883) and a grant (20SCIP-B105148-06) from the Construction Technology Research Program, funded by the Ministry of Land, Infrastructure, and Transport (MOLIT) of the Korean government.

References

Chen, J.Y., Sun, S.N. and Wang, B.G. (2008), "Dynamic analysis for the tether of submerged floating tunnel", *Chin. J. Comput. Mech.*, **25**(4), 488-493.

Do, N.A., Dias, D. and Oreste, P. (2018), "Numerical investigation of segmental tunnel linings-comparison between the hyperstatic reaction method and a 3D numerical model", *Geomech. Eng.*, **14**(3), 293-299. https://doi.org/10.12989/gae.2018.14.3.293.

Hong, Y. and Ge, F. (2010), "Dynamic response and structural integrity of submerged floating tunnel due to hydrodynamic load and accidental load", *Proc. Eng.*, **4**, 35-50. https://doi.org/10.1016/j.proeng.2010.08.006.

Itasca, F. (2013), *Fast Lagrangian Analysis of Continua in 3 Dimensions*. Online Manual.

Jakobsen, B. (2010), "Design of the Submerged Floating Tunnel operating under various conditions", *Proc. Eng.*, **4**, 71-79. https://doi.org/10.1016/j.proeng.2010.08.009.

Jin, C. and Kim, M. (2017), "Dynamic and structural responses of a submerged floating tunnel under extreme wave conditions", *Ocean Syst. Eng.*, **7**(4), 413-433. https://doi.org/10.12989/ose.2017.7.4.413.

Kunisu, H., Mizuno, S., Mizuno, Y. and Saeki, H. (1994), "Study on submerged floating tunnel characteristics under the wave condition", *Proceedings of the 4th International Offshore and Polar Engineering Conference*, Osaka, Japan, April.

Lee, J.Y., Jin, C. and Kim, M. (2017), "Dynamic response analysis of submerged floating tunnels by wave and seismic excitations", *Ocean Syst. Eng.*, **7**(1), 1-19. https://doi.org/10.12989/ose.2017.7.1.001.

Mazzolani, F.M., Faggiano, B. and Martire, G. (2010), "Design aspects of the AB prototype in the Qiandao Lake", *Proc. Eng.*, **4**, 21-33. https://doi.org/10.1016/j.proeng.2010.08.005.

Nilsen, B. and Palmstrøm, A. (2001), "Stability and water leakage of hard rock subsea tunnels", *Modern Tunn. Sci. Technol.*, 497502.

Oh, S.H., Park, W.S., Jang, S.C. and Kim, D.H. (2013), "Investigation on the behavioral and hydrodynamic characteristics of submerged floating tunnel based on regular wave experiments", *J. Kor. Soc. Civ. Eng.*, **33**(5), 1887-1895. https://doi.org/10.12652/Ksce.2013.33.5.1887.

Shi, P., Zhang, D., Pan, J. and Liu, W. (2016), "Geological investigation and tunnel excavation aspects of the weakness zones of Xiang'an subsea tunnels in China", *Rock Mech. Rock Eng.*, **49**(12), 4853-4867. https://doi.org/10.1007/s00603-016-1076-z.

Xiao, J. and Huang, G. (2010), "Transverse earthquake response and design analysis of submerged floating tunnels with various shore connections", *Proc. Eng.*, **4**, 233-242. https://doi.org/10.1016/j.proeng.2010.08.027.

Yan, H., Luo, Y. and Yu, J. (2016), "Dynamic response of submerged floating tunnel in the flow field", *Proc. Eng.*, **166**, 107-117. https://doi.org/10.1016/j.proeng.2016.11.573.

Yarramsetty, P.C.R., Domala, V., Poluraju, P. and Sharma, R. (2019), "A study on response analysis of submerged floating tunnel with linear and nonlinear cables", *Ocean Syst. Eng.*, **9**(3), 219-240. https://doi.org/10.12989/ose.2019.9.3.219.

Youshi, H. and Fei, G. (2010), "Dynamic response and structural integrity of submerged floating", *Proc. Eng.*, **4**, 35-50. https://doi.org/10.1016/j.proeng.2010.08.006.

Zhang, J., Li, S., Li, L., Zhang, Q., Xu, Z., Wu, J. and He, P. (2017), "Grouting effects evaluation of water-rich faults and its engineering application in Qingdao Jiaozhou Bay Subsea Tunnel, China", *Geomech. Eng.*, **12**(1), 35-52. https://doi.org/10.12989/gae.2017.12.1.035.

Zhang, K., Xiang, Y. and Du, Y. (2010), "Research on tubular segment design of submerged floating tunnel", *Proc. Eng.*, **4**, 199-205. https://doi.org/10.1016/j.proeng.2010.08.023.

Zhou, X.J., Wang, Z.Y., Fan, Y.H. and Pan, J. (2012), "Safety study on connection joint for submerged floating tunnel", *Appl. Mech. Mater.*, **170**, 1708-1711. https://doi.org/10.4028/www.scientific.net/AMM.170-173.1708.

Zingg, S. and Anagnostou, G. (2012), "Tunnel face stability in narrow water-bearing fault zones", *Proceedings of the EUROCK 2012, the 2012 ISRM International Symposium-Rock Engineering and Technology for Sustainable Underground Construction*, Stockholm, Sweden, May.

CC